INTERNATIONAL JOURNAL FOR NUMERICAL METHODS IN FLUIDS
*Int. J. Numer. Meth. Fluids* 2002; **39**:343–359 (DOI: 10.1002/fld.340)

# Simulations of high-aspect-ratio jets

A. E. Holdø*,† and B. A. F. Simpson

*Department of Aerospace, Civil and Mechanical Engineering, University of Hertfordshire, College Lane, Hatfield AL10 9AB, England, U.K.*

SUMMARY

There are many practical situations when jets are emanating from non-axis-symmetric apertures, yet numerical simulations of such three-dimensional jets are scarce and most of them have failed to reproduce some of the unique flow features. Examples of this type of jets are gas leaks from flanges. These can be treated as jets issuing from high aspect ratio rectangular orifices. The present work consists of a series of large eddy simulations typifying such jets using different inflow boundary conditions. Good agreement with available experiments was observed provided appropriate boundary conditions were present.

A discrete method for formulating turbulence data with a known energy spectrum for an inflow condition is outlined and evaluated with three other inflow conditions—a steady uniform profile, a steady parabolic profile and pseudo-random noise. The implementation of the new inlet condition results in a more realistic centreline velocity decay where the division between the end of the potential core region and the start of the characteristic decay region is clearly visible. Large velocity oscillations are also observed in the final quarter of the domain (15–20 slot widths downstream). Similar oscillations have been observed in real jets. Off-centre mean velocity peaks are present along the major axis 10 slot widths downstream of the exit in all the simulations. The peaks are approximately 3% of the centreline velocity. The presence of the off-centre peaks are proved to be independent of jet inflow boundary conditions and an explanation for the mechanism causing the off-centre peaks is given. Copyright © 2002 John Wiley & Sons, Ltd.

## 1. INTRODUCTION

Jets are present in many industrial systems and applications. The jets may be designed for specific functions or they may be present due to system failure. In many cases jets emanate from specifically designed orifices and in such cases the orifices are nearly always of an axis-symmetric design. However, in the case of jets caused by rupture of seals or gaskets the resulting jets are unlikely to issue from smooth, axis-symmetric orifices. Properties for jets that are not issuing from circular cross-section apertures are not so well documented

*Correspondence to: A. E. Holdø, Aerospace, Civil and Mechanical Engineering, University of Hertfordshire, Hatfield Campus, College Lane, Hatfield, Herts AL10 9AB, England, U.K.
†E-mail: a.e.holdo@herts.ac.uk

Contract/grant sponsor: Engineering and Physical Science Research Council; contract/grant number: GR/J77108/01.

*Received February 2001*
*Revised November 2001*

Copyright © 2002 John Wiley & Sons, Ltd.

due to the smaller number of studies of such jets [1]. Simulations of this type of jet using computational fluid dynamics (CFD) have also appeared to be difficult [2]. One example where these jets are present is in the offshore oil and gas industry. Parts of oil and gas production installations consist of pipelines carrying flammable hydrocarbon gases. These installations are frequently subjected to extreme environmental and operational conditions. The pipe networks are often very complex, built in sections and interconnected with additional components such as junctions, reservoirs and pumps. It is the nature of these networks that any connection is a potential leakage source [15]. A statistically likely scenario is a leak from a damaged flange joint. The jet issuing from a damaged flange joint would initially have a non-circular cross-section. Furthermore, the state of flow at the leak is unlikely to be known in any detail. The present techniques used for safety assessments related to such leakage are based on information from experimental and numerical axis-symmetric jet studies. However, a flange leakage will be partially annular in form and is from an initial geometric point of view better treated as a rectangular jet with a high aspect ratio. In the current work an orifice is described, as having a high aspect ratio if the width of the orifice divided by its height is 10 or greater. The main objective of the present work was to investigate how well such jets could be simulated using CFD techniques.

Three-dimensional, incompressible turbulent jets are quite complex flow structures as shown in Figure 1. However, their time-averaged properties are characterized by the presence of three distinct regions in the flow direction. The regions are named after the decay rate along the centre line of the jet. The regions are named the potential core region, the characteristic decay region and the axis-symmetric decay region. Figure 2 shows the presence of these regions for a jet issuing from a high aspect ratio orifice.

A gas leakage in an offshore module that contains a complex pipe system is likely to be impeded before the final axis-symmetric region ever develops. Therefore, it is important to study the behaviour of the jet in the near field where the orifice geometry has a large effect on the flow field [3].

Experimental investigators have identified several unique flow features associated with rectangular jets issuing from sharp edged orifices. Specifically in the near field, a vena contracta and off-centre velocity peaks (saddle-backed velocity profiles) develop along the major axis. The vena contracta is a consequence of the curvature of the streamlines that occurs as the fluid passes through the orifice. Although the off-centre velocity peaks were observed three decades ago [3] they are still not well understood.

Very few numerical simulations have been attempted of three-dimensional turbulent jets issuing from rectangular orifices. Simulations that have employed two-equation turbulence models have in the most been unsuccessful. To reproduce the vena contracta, cross-stream velocities have had to be specified in a somewhat arbitrary way at the jet exit and the simulations have completely failed to reproduce the reported saddle-backed velocity profiles [2] or 'dog-bone' velocity contours in the plane normal to the jet axis. Recent work using large eddy simulations (LES) based on the Smagorinsky sub-grid scale turbulence model has shown that in contrast to the two-equation turbulence model-based simulations, saddle-backed velocity profiles could be reproduced in a LES of a jet issuing from high aspect ratio orifice [4]. However, this work employed a uniform velocity profile at the inlet boundary with no attempt to model the turbulence, which would be present in a real life application. Modelling of turbulence and shear at inflow boundaries has also been demonstrated to be important even when using two-equation type turbulence models [5]. This has prompted the current

Copyright © 2002 John Wiley & Sons, Ltd. 

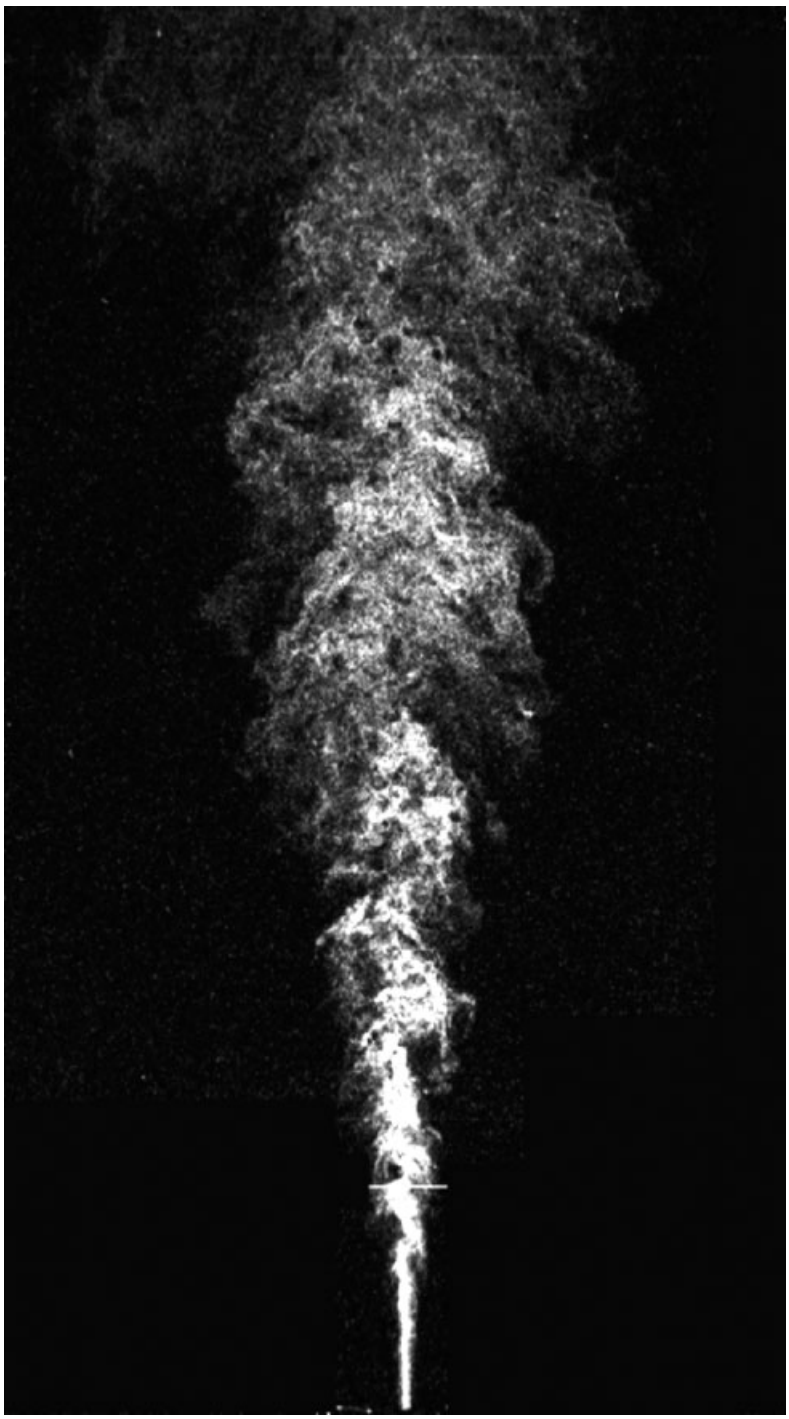

Figure 1. A photograph of a three-dimensional turbulent gas leak jet. The view is of the minor axis and the jet, with a Reynolds number of 33 500, is issuing from an orifice of 40:1 ratio [6, 16, 17].

Copyright © 2002 John Wiley & Sons, Ltd. 

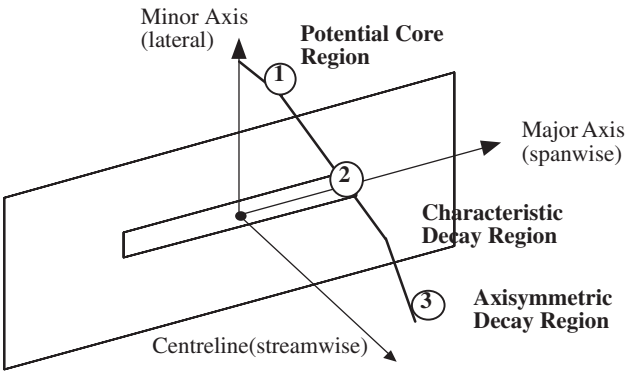


Figure 2. Rectangular jet configuration showing the centre line velocity decay regions which characterize a jet issuing from a rectangular cross-section orifice. Regions 1, 2 and 3 illustrates the centerline velocity decay of the jet.

investigation into the effect of inflow boundary conditions on the LES simulation of jet flow, both in terms of mean shear profiles and turbulence prescription. The results of this study are also important for the industrial application of LES simulations since turbulence conditions of a flow entering a domain of interest may not always be known. In many circumstances for academic studies another simulation is carried out prior to the main simulation in order to establish turbulence data. This is not practical for industrial applications and an important additional aim of the present study was to develop a framework for prescribing turbulence conditions at an inlet to a domain when using LES-based turbulence modelling techniques.

## 2. NUMERICAL METHODS

Experimental evidence from studies of three-dimensional jets (Figure 1) illustrate that the complex turbulent flow in the near field of a high Reynolds number non-axis-symmetric jet is non-symmetric, unsteady and non-isotropic [6, 7]. Consequently, a simulation of the flow will have to be three-dimensional and time-dependent to allow the jet to develop in space and through time.

### *2.1. Governing equations*

In the present study only conservation of momentum and mass were applied as the flows were assumed to be in the incompressible range and without any heat transfer. In order to use LES-based turbulence modelling, it is necessary to perform spatial averaging of the governing equations. This is in contrast to turbulence modelling based on the two-equation models, which are derived from the time-averaged governing equations. These turbulence models are sometimes referred to as Reynolds-averaged Navier–Stokes-based models or RANS-based models.

In order to obtain the basis for LES, the partial differential equations governing the large-scale motion can be obtained by applying a spatial filter (indicated by the over bar) to the

Copyright © 2002 John Wiley & Sons, Ltd. 

Navier–Stokes and continuity equations. This gives rise to the so-called sub-grid stresses which can be expressed as

$$\tau_{ij} = -2\mu_s S_{ij} \tag{1}$$

where $\mu_s$ is the eddy viscosity calculated by the Smagorinsky model given as

$$\mu_s = (\mathrm{Cs} \cdot \Delta)^2 \left( \frac{1}{2} \overline{S_{ij} S_{ij}} \right)^{1/2} \tag{2}$$

where $S_{ij}$ is the strain rate tensor of the resolved field, Cs is the Smagorinsky constant whose value is taken to be 0.17 for all of the present calculations and $\Delta$ is the characteristic sub-grid length scale which is selected as

$$\Delta = (\Delta_x \Delta_y \Delta_z)^{1/3} \tag{3}$$

Hence the length scale is directly calculated from the local grid size. The calculation of the sub-grid viscosity is performed using a subroutine that returns an array of values at each time step.

### 2.2. *Spatial and temporal discretization*

In the present simulations, a general purpose finite element code Reference [8] was used in conjunction with the relatively universal Smagorinsky sub-grid scale turbulence model to obtain a solution for the spatially-averaged Navier–Stokes equations. The finite element method is inherently implicit and involves a high degree of coupling between the governing equations. However, the solution methodology employed involved the solving of each equation in a segregated, sequential manner. The current work used a second-order semi-implicit time-advancement scheme to ensure a stable and accurate solution.

## 3. MODEL DETAILS

### 3.1. *Jet configuration*

Simulations were performed for a single isothermal, incompressible, three-dimensional jet of air issuing perpendicularly from a 10:1 aspect ratio orifice into ambient air. The flow geometry used (Figure 3) was previously investigated experimentally by Quinn *et al.* [9].

### 3.2. *Computational grid*

In order to resolve the structures in the free shear layers and still cover a relatively large flow domain a non-uniform mesh was used. The rectangular mesh was refined in the vicinity of the jet exit and smoothly expanded towards the entrainment and outflow boundaries. The expansion ratios lie between 0.6 and 1.6 in all directions. This ensured a fine mesh in the regions where high velocity gradients were expected, but with possible penalties in terms of increased numerical diffusion in the regions of lower mesh density and the highest expansion ratios. For all mesh sizes the number of mesh points in the shorter cross-stream dimension of the domain (Figure 3) were the same as in the stream-wise direction, but the mesh point

Copyright © 2002 John Wiley & Sons, Ltd. 

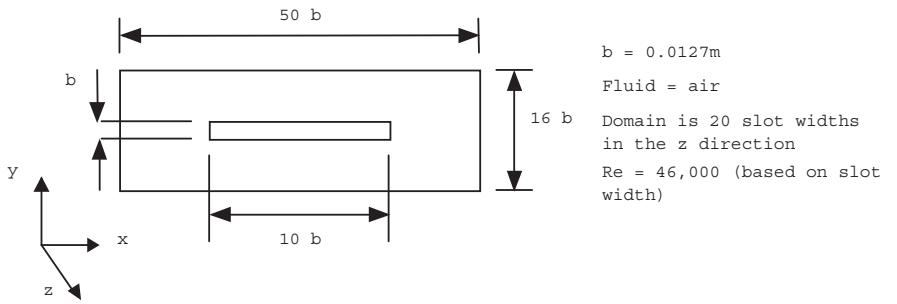


Figure 3. Inlet plate geometry with co-ordinate directions used in the present study.

number was smaller by a factor of 2.5 than the number of mesh points in the larger cross-stream dimension. One of the wider aims of the present work was to investigate the necessity of having extremely fine grids, which is a reason why LES has traditionally been regarded as inaccessible. Even with complex high Reynolds number flows it is desirable to have only the locally isotropic smaller dissipative scales being modelled by the sub-grid turbulence model. However, it is not always practical to have a grid that resolves to these scales at all locations and a coarser grid is used. In these cases the simulations are often termed very large eddy simulations (VLES) and ideally a more sophisticated sub-grid model than the Smagorinsky model should be employed. Three different sized grids were used in the present work. The coarser grid of 68 820 nodes is more manageable and is classified as a VLES. The medium grid has 126 000 nodes and the finer grid of 307 000 nodes is classified as a LES. However, each VLES simulation still required in excess of 100 h to complete when running on an IBM RS 6000 machine with 512 Mb of memory. All cases reported in the present paper are based on the LES grid, but even for this grid it is unlikely that only the locally isotropic smaller dissipative scales were the largest scales modelled by the Smagorinsky model as the Kolmogorov scale for the present study was estimated to be of the order of 0.01 mm for the present case which is two orders of magnitude smaller than the smallest mesh cell used. The VLES simulations were used as 'pump-priming' exercises.

### *3.3. Time advancement*

A reference case of 200 time steps of 0.001 s was established for the VLES simulation. This time step is also large (as are the mesh cells) compared with the smaller dissipative scales. The 'flow-through time' based on the time-mean velocity is 0.005 s. At least 5 flow-through times of the computational domain were run (25 time steps) to allow numerical transients to pass through the domain before the remaining simulation results were time averaged.

### *3.4. Boundary conditions*

Inflow and outflow boundary conditions pose particularly severe difficulties when a fully turbulent flow prevails. This is because detailed knowledge is required about the state of the flow at the edge of the domain. It is not possible to use periodic boundary conditions because the flow to be studied is evolving in space and time in all co-ordinate directions. Some researchers in the past have explicitly provided three-dimensional and time-dependent

Copyright © 2002 John Wiley & Sons, Ltd. 

data with secondary computations. This requires additional CPU time and excessive data management and storage capacity. In the present study four inlet conditions were used:

- A uniform, steady velocity profile.
- A profiled, steady velocity profile.
- A uniform profile with pseudo-random noise superimposed.
- A uniform velocity profile with turbulent fluctuations generated by inverse fast Fourier transform (FFT) superimposed.

The first simulation employed a simple top hat inlet velocity profile. This is the same as the condition described in the introduction and used by Simpson *et al.* [4]. This boundary condition does not represent the turbulent intensities that would be present in a real jet with a Reynolds number of 46 000 and the starting boundary layers at the jet exit are presumed not to be present as the top hat velocity profile represents no viscous losses prior to the start of the jet. Another consequence of using a top hat profile at the inlet is the development of very sharp and unrealistic velocity gradients at the edges of the orifice. This leads to unrealistic sub-grid viscosities. Through inspection of Equation (2) it is seen that the sub-grid viscosities depend directly on the local velocity gradients.

A profiled velocity profile was used in the second simulation in order to reduce the possible over specification of sub-grid viscosity at the inlet through the use of the top hat velocity profile. Whilst a profiled velocity distribution does not represent the fluctuations in a fully developed turbulent flow, it reduces the sub-grid viscosity at the edges of the inlet compared to the top hat profile. The following expression was used to define the profile:

$$\frac{w}{w_{\mathrm{cl}}} = \left(1 - \frac{2r}{d}\right)^{1/7} \tag{4}$$

The above expression refers to an axis-symmetric case, whilst in the present case the slot width $b$ would be the constant rather than the diameter $d$.

The mass flow through the inlet was kept constant in the profiled velocity distribution case compared to the other three cases. However, it has been observed that small changes in the Reynolds number has very little effect on the flow features of three-dimensional jets at the Reynolds numbers subject to the present study [9].

Neither the first nor the second inlet condition case made any effort to simulate or generate turbulence at the inlet. If the flow is turbulent at the inlet as is the case of the present study then to maintain turbulence throughout the flow, turbulent kinetic energy should be continuously supplied by the inlet condition. Therefore, a simple time-mean inlet condition is an inadequate inlet boundary condition for a time-dependent LES simulation. The third and fourth simulations attempted to overcome this deficiency by superimposing small amplitude time-dependent velocity fluctuations on to a steady uniform profile. To simplify the simulation the turbulence upstream of the jet exit was assumed to be isotropic. It was also noted that experimental investigators of three-dimensional turbulent jets have recorded turbulence intensities at the jet exit of between 0.7 and 5.0% of the centreline stream wise velocity [6, 7].

In the third case, it was assumed that the turbulent velocity fluctuations could be supplied in any format as long as they generated turbulent kinetic energy. This is similar in concept to the approach taken by Holdø and Weibust [10] for triggering vortex shedding. Consequently,

Copyright © 2002 John Wiley & Sons, Ltd. 

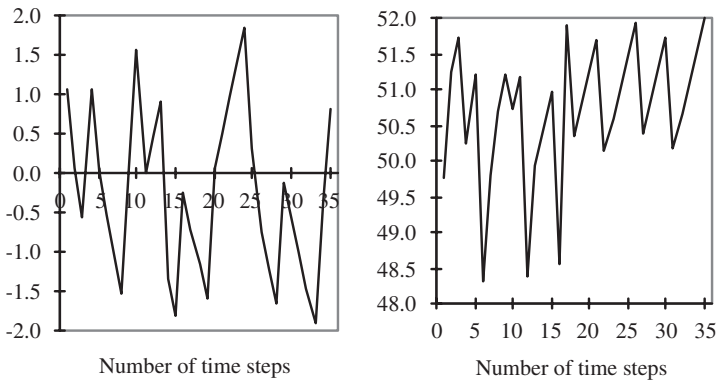


Figure 4. Velocity components in the $x$ and $z$ directions shown as functions of time (time step). Velocity magnitude is in m/s. Measurements are taken at a node at jet exit and the pseudo-random inlet boundary condition was used.

the turbulent velocity fluctuations were simulated using pseudo-randomly produced noise. An example of the $z$ velocity component and $x$ velocity component is given in Figure 4. The graphs show that the time mean velocity in the stream wise direction is 50 m/s and in the span wise direction is 0 m/s. The time-mean velocity in the lateral direction is also zero.

In the fourth case it was assumed that the turbulence fluctuations had to resemble a realistic turbulent flow. In order to achieve this, a method similar to the one developed by Lee *et al.* [11] was devised. The approach presented here uses a more general three-dimensional normalized energy spectra as the target spectra. It is known that the area under the energy/frequency spectra is proportional to the turbulent intensity. In this method discrete frequencies representing bandwidths are selected and the turbulent kinetic energy for each of them is calculated. These frequencies and their corresponding energy values are then summated in a Fourier series to construct an input signal. The signal was shifted between each node (along the inflow boundary) and co-ordinate direction ($X$, $Y$ and $Z$) by a subtle change in the phase shift, $T$. This change was introduced by multiplying a constant value designated to each node, by a pseudo-random number generated by the computer using a seed and by the clock time on the machine. This elaborate number generating methodology was employed to make the phase shift as chaotic as possible. The resulting input signal was one possible turbulent signal in an infinite set and each time the problem was run a different turbulent input signal was generated.

This inlet condition has several advantages. Firstly no additional simulations are needed and in this respect it is relatively computationally inexpensive. Secondly the turbulent signal will have the correct characteristic energy spectra and thirdly anisotropic turbulence can be introduced by allowing different sized intensities to govern the limits of the incoming signal. The only difficulty would lie in retaining the correlation between the velocity fluctuations in the three co-ordinate directions.

Examples of the velocity component fluctuations generated in this manner in the $x, y, z$ directions are given in Figure 5. The spectrum presented in Figure 6 was constructed by performing a fast Fourier transform on one of the velocity components at the jet exit in case 4.

Copyright © 2002 John Wiley & Sons, Ltd. 

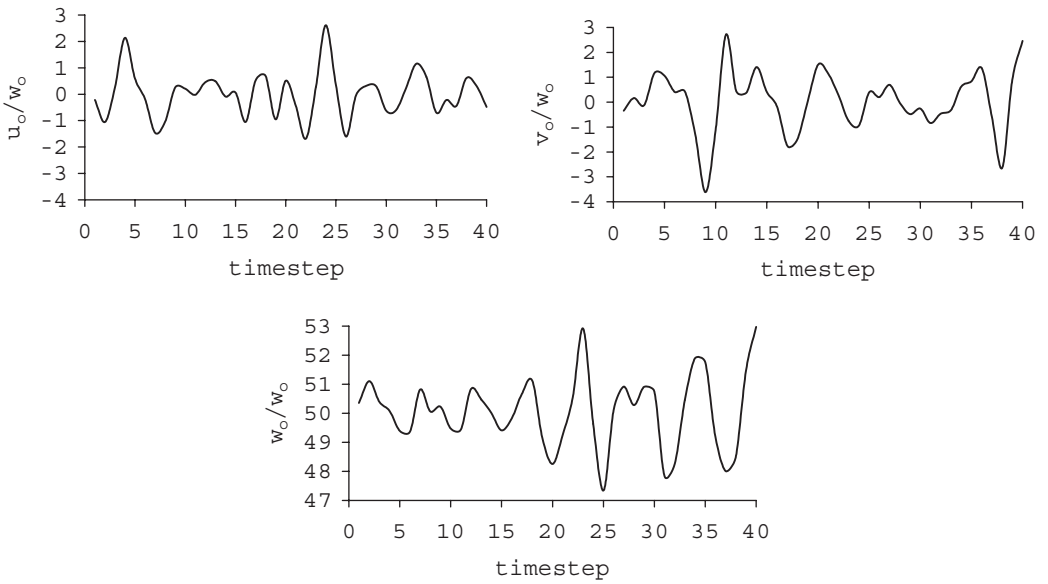


Figure 5. Velocity components in the $x$, $y$ and $z$ directions as a function of time. Measurements are taken at a node at the jet exit and the inflow turbulence condition with a known energy spectrum was used. Each time step is 0.001 s and the mean inlet velocity is 50 m/s in the stream-wise direction and zero in the other two. The turbulence at the inlet is assumed isotropic and with an intensity of 2%.

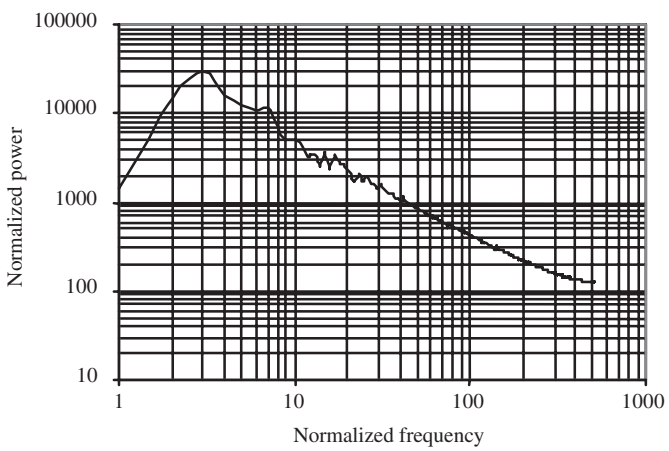


Figure 6. Power spectrum for the known energy spectrum inlet condition.

The spectrum of the velocity component is very similar to the original three-dimensional spectra decomposed to construct the signal in the first place. However, the tail end of the spectrum breaks away from the $-\frac{5}{3}$ Kolmogorov log law in the so-called inertial subrange because the sampling rate at the higher frequencies was very low.

Copyright © 2002 John Wiley & Sons, Ltd. 

A proper outflow condition allows the flow to pass through the exit boundary with little distortion, so that the interior solution is not polluted by errors from the exit boundary [12]. Zero stress conditions were set at the outflow and entrainment boundaries.

## 4. RESULTS AND DISCUSSION

A first assessment of the development of the jet through the flow domain can be gauged by examining the velocity decay along the centreline. Figure 7 shows a comparison of the centreline velocity decays between the LES with the different inlet boundary conditions. The centreline velocities are all time-averaged and normalized with the time-mean centreline velocity at the jet exit. The distance downstream is measured in slot widths.

The decay curves in the first three cases are similar and it is difficult to identify the regions in the jet. In these cases the centreline velocity is approximately proportional to the log of the distance downstream all the way to 20 slot widths. In contrast the simulation with the turbulent inflow that has a known energy spectrum has clearly defined regions, which are in good agreement with the experimental values of Quinn *et al.* [9]. The potential core region finishes after approximately 3 slot widths. After $z/b = 3$ there follows a typical second decay region that begins with a slow acceleration in the rate of decay of the centreline stream wise velocity until $z/b = 10$. From this point the decay rate is closer to a constant value and approximately equal to $z^{-0.34}$. An explanation for this difference between the results of varying inflow boundary conditions can be found through the variation in centreline turbulence. The centreline turbulence intensity results are illustrated in Figure 8(a)–8(c). It is readily seen that there is agreement between the turbulence intensities from experiment and the turbulent numerical inlet, whilst for all other cases the turbulence intensities are substantially lower than for the experimental case. Whilst the turbulence intensities are not directly responsible for differences in velocity decay, the results in Figure 8(a)–8(c) shows the importance of

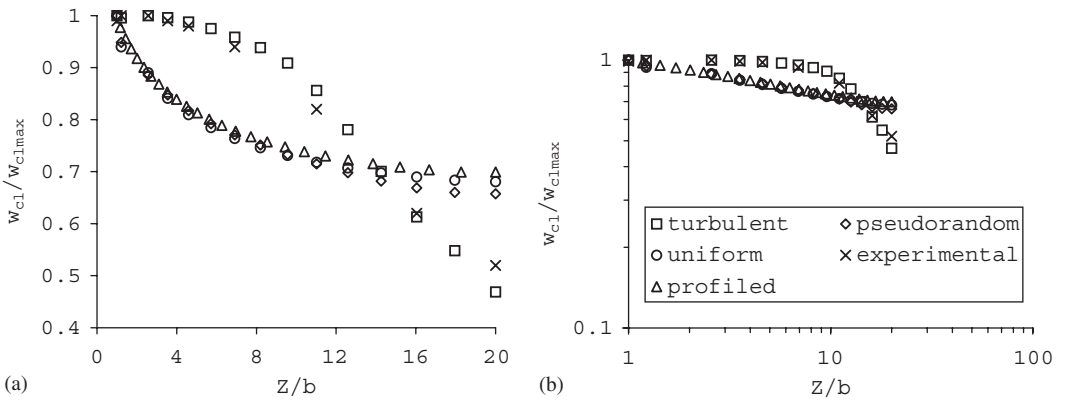


Figure 7. (a) Mean stream-wise velocity decay along the centreline of a turbulent three-dimensional jet. A comparison between LES with differing inlet boundary conditions and the experimental results of Quinn *et al.* [9]. (b) Mean stream-wise velocity decay along the centreline of a turbulent three-dimensional jet. A comparison between LES with differing inlet boundary conditions and the experimental results of Quinn *et al.* [9]. Logarithmic axis.

Copyright © 2002 John Wiley & Sons, Ltd. 

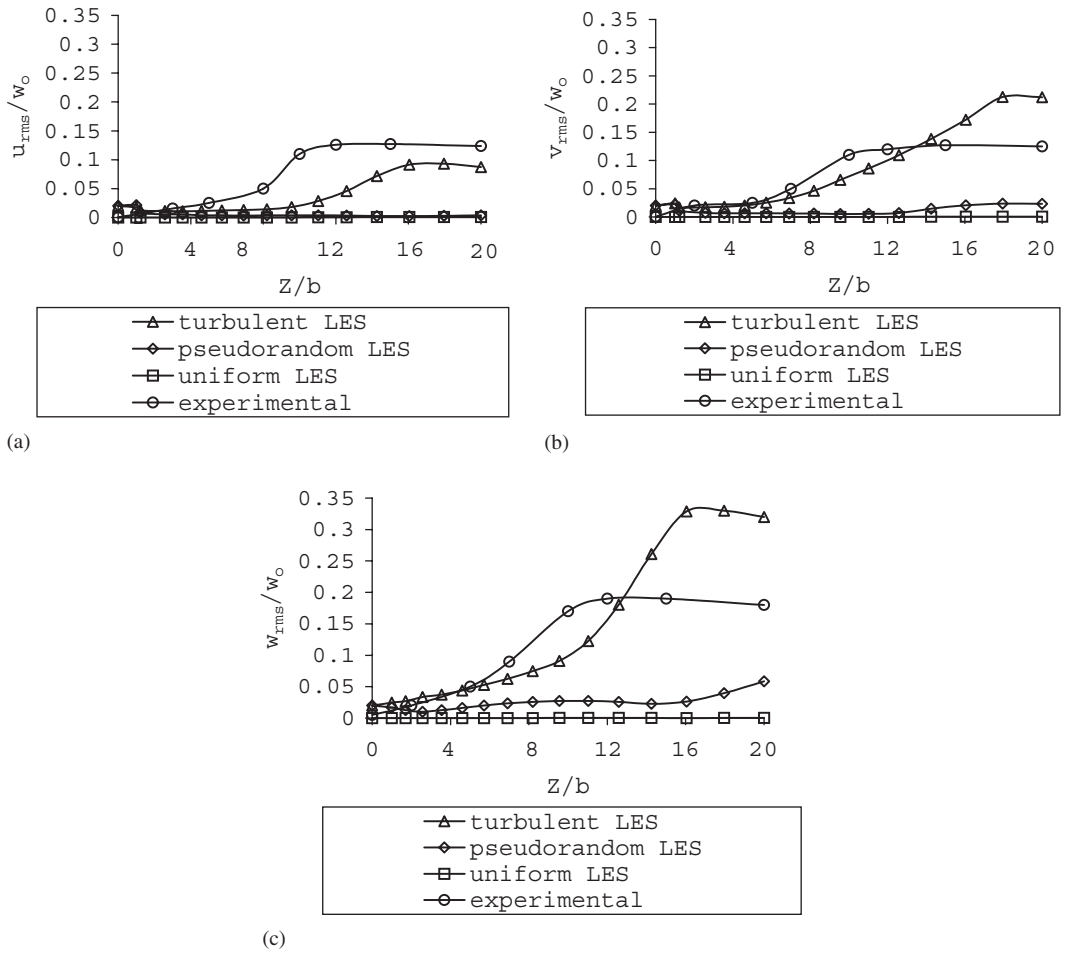


Figure 8. (a) Variation of the spanwise grid scale turbulence intensity along the centreline of the jet, compared to the experimental data of Quinn *et al.* [9]. (b) Variation of the lateral grid scale turbulence intensity along the centreline of the jet, compared to the experimental data of Quinn *et al.* [9]. (c) Variation of the streamwise grid scale turbulence intensity along the centreline of the jet, compared to the experimental data of Quinn *et al.* [9].

using a turbulent inlet in order to achieve reasonable agreement with experiments. This result shows the discrepancies between the experimental turbulence intensity values and the cases with pseudorandom and uniform inlet flow conditions to be between 0.1 and 0.15, which is a considerable difference given that the level of the experimental values are of the same magnitude. The next assessment of jet development is related to the jet spread with downstream distance. The results from the turbulent inflow that has a known energy spectrum are compared with experimental studies as shown in Figure 9. The half widths in the $y$ direction are found to generally decrease in the domain, whilst the half widths in the $x$ direction are constant for the first few slot width and then begin to increase with a constant spreading

Copyright © 2002 John Wiley & Sons, Ltd. 

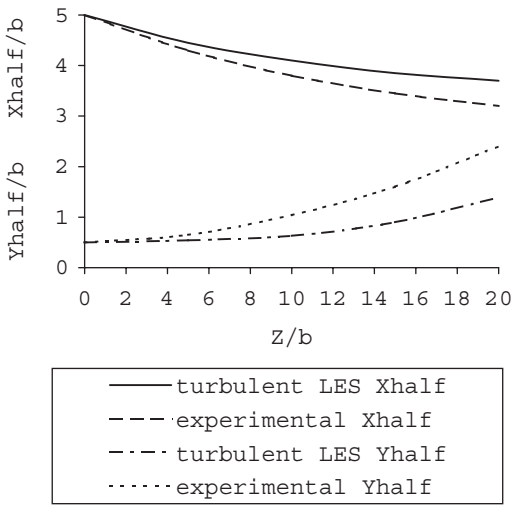


Figure 9. Growth of the Jet (spread) with downstream distance in the *XZ* and *YZ* planes. Comparison with experiments of Quinn *et al.* [9].

rate. It is also seen that whilst there is agreement between experimental and numerical values for the first 6 slot width (difference between experimental and calculated values within 5% of a slot width), there is an increasing difference between the results from 6 slot width onwards. The experimental curves show an increase in growth in the $x$ direction and a decrease in growth in the $y$ direction compared to the computed values. An important factor in the growth of the jet is turbulence and since shear is in general important for jets, the turbulent shear stresses (or Reynolds stresses) are significant features. To examine the numerical results in this respect, the time-averaged values of the velocity fluctuations and their correlations (or Reynolds stresses) were examined.

Figure 10(a)–10(d) shows a comparison between experimental and numerical results in the *xz* and *yz* planes at the downstream distances of 10 and 20 slot widths in terms of turbulent kinetic energy and Reynolds stresses. The results show that there is a difference between experiment and computation in location of maximum value for both the quantities in the *xz* plane. Whilst the locations of the maxima are different between experiment and computation, the values are on average of the same magnitude. This could partly explain the higher spreading rate of the jet in the *xz* plane for the numerical simulation. A similar situation is seen in the *yz* plane, however, here the maximum values of the turbulent kinetic energy and the Reynolds stress are significantly higher for the computational study on average, but not near the jet edges. Both the differences in stress and kinetic energy is likely to be influenced by the coarsening of the mesh in all directions (relative to jet boundary) with downstream distance. The difference in Reynolds stress in particular will influence the spreading rate.

Whilst the differing inflow conditions gave rise to differing development of the jet and the turbulent inflow from the known energy spectrum gave the results closest to experimental values, it was found that all inflow conditions gave a so-called saddle back velocity profiles. The best agreement between simulation and experiment was found for the turbulent inlet case

Copyright © 2002 John Wiley & Sons, Ltd. 

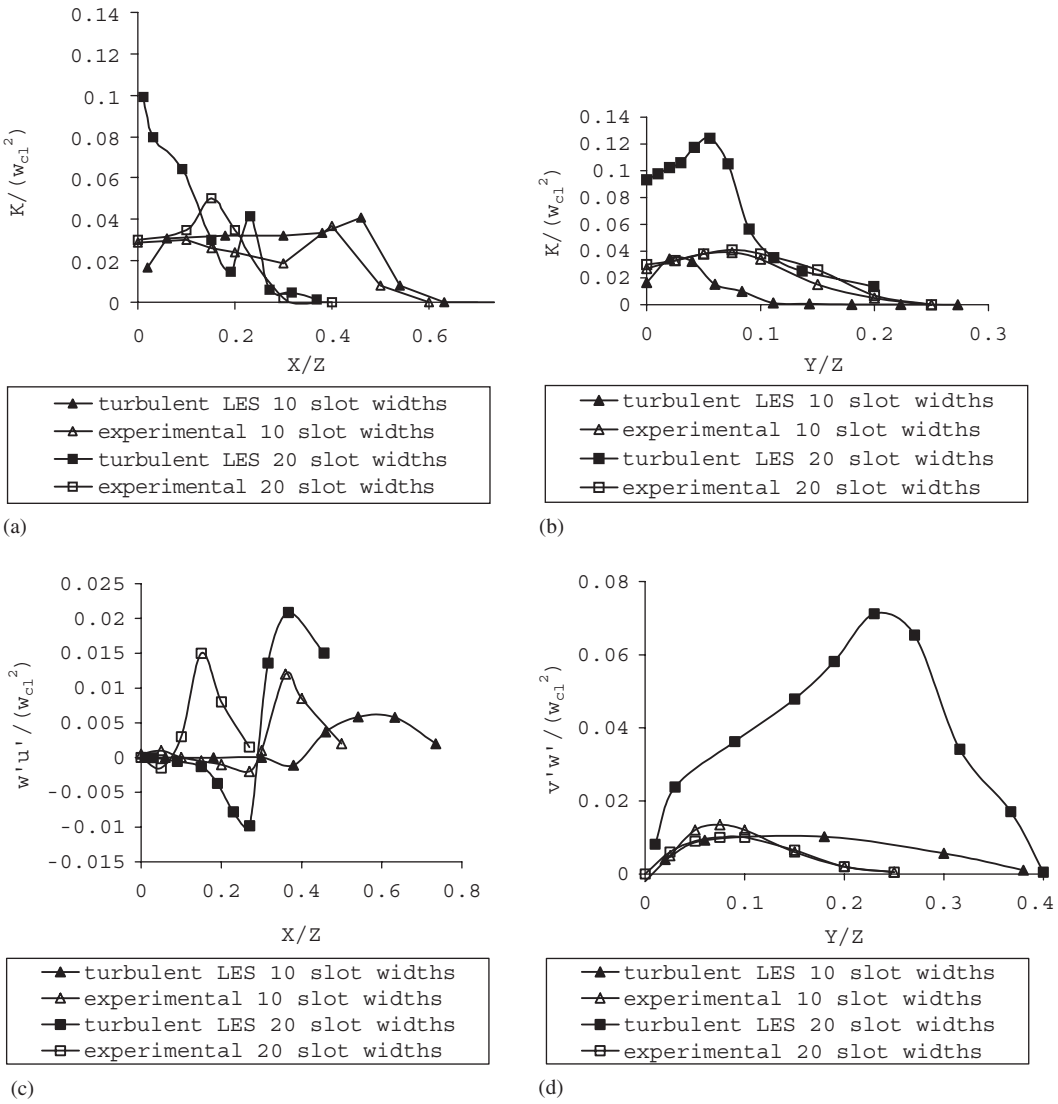


Figure 10. (a) Grid scale turbulent kinetic energy profiles in the $XZ$ plane at $Y/b = 0$ compared to the experimental data of Quinn *et al.* [9]. (b) Grid scale turbulent kinetic energy profiles in the $YZ$ plane at $X/b = 0$ compared to the experimental data of Quinn *et al.* [9]. (c) Grid scale turbulent shear stress profiles in the $XZ$ plane at $Y/b = 0$, compared to the experimental data of Quinn *et al.* [9]. (d) Grid scale turbulent shear stress profiles in the $YZ$ plane, compared to the experimental data of Quinn *et al.* [9].

(Figure 11). This is in contrast to the arguments of McQuirk and Rodi [2] and Pollard and Schwab [13] who suggest that the saddle back velocity profile results from boundary layer interaction inside the settling chamber upstream of the orifice. The present work with the

Copyright © 2002 John Wiley & Sons, Ltd. 

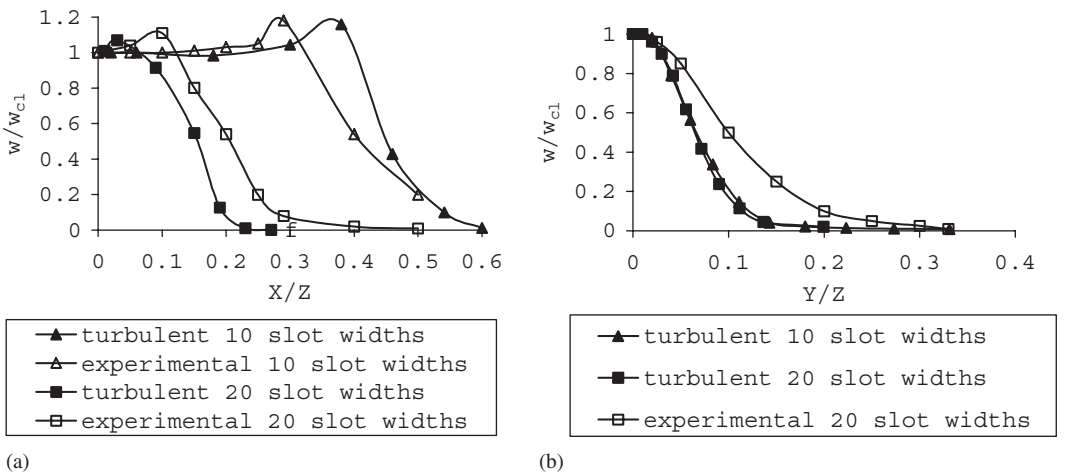


Figure 11. Comparison between the turbulent inlet LES and the experimental results of Quinn *et al.* [9]. The mean stream-wise velocity profiles in the *XZ* plane.

differing inlet velocity profiles and turbulence conditions illustrates that this cannot be the case since the saddle back is present for all simulations. Instead it is believed that the profiles are formed by mechanisms resulting from the entrained fluid entering the jet flow normal to the jet stream wise axis. The resulting curvature of the streamlines of the entrained fluid will be severe and the fluid particles will experience normal accelerations towards the centre of curvature, Simpson *et al.* [4]. This hypothesis is supported by investigations of jets issuing from long channels Sfeir [14]. In these cases, the entrained field does not enter normal to the stream wise axis and off-centre velocity peaks are not observed. A test of this hypothesis was also carried out through testing the jets with different conditions for the orifice wall (*xy* plane at outlet). Three different conditions were tested. These were a 'no-slip' condition, frictionless wall and no-wall. The results in terms of saddle backed profiles are seen from Figure 12. Whilst the no-slip and frictionless wall which both give streamline curvature the results show saddle backed velocity profiles as predicted, but the no-wall condition does not yield a saddle back result, also as predicted. However, the peaks are only 3% of the mean centre line velocity and not 6% as found from experiments [9]. This suggests that the numerical dissipation or possibly the Smagorinsky constant may be too large for high gradients.

A further phenomenon related to high aspect ratio jets is the jet flapping. This is illustrated by Figure 13 and has been observed from experiments. However, for the present study, jet flapping was only observed for the turbulent inlet boundary condition.

The results clearly illustrate the need for appropriate turbulence inlet boundary conditions. The important finding of the present study is that the turbulence boundary condition has to emulate the effect in terms of velocity fluctuations on the boundary of real turbulence. It is clearly demonstrated that even the correct turbulence intensity, but prescribed as a pseudo-random signal is inadequate to trigger the appropriate mechanisms. This is a matter for further investigation.

Copyright © 2002 John Wiley & Sons, Ltd. 

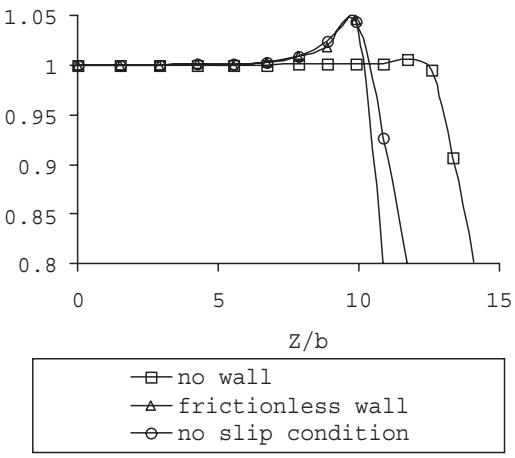


Figure 12. Investigation of the effect that the wall condition around the jet exit has on the mean stream-wise velocity profiles in the $Z$–$X$ plane. Stream-wise velocity component against distance from centreline.

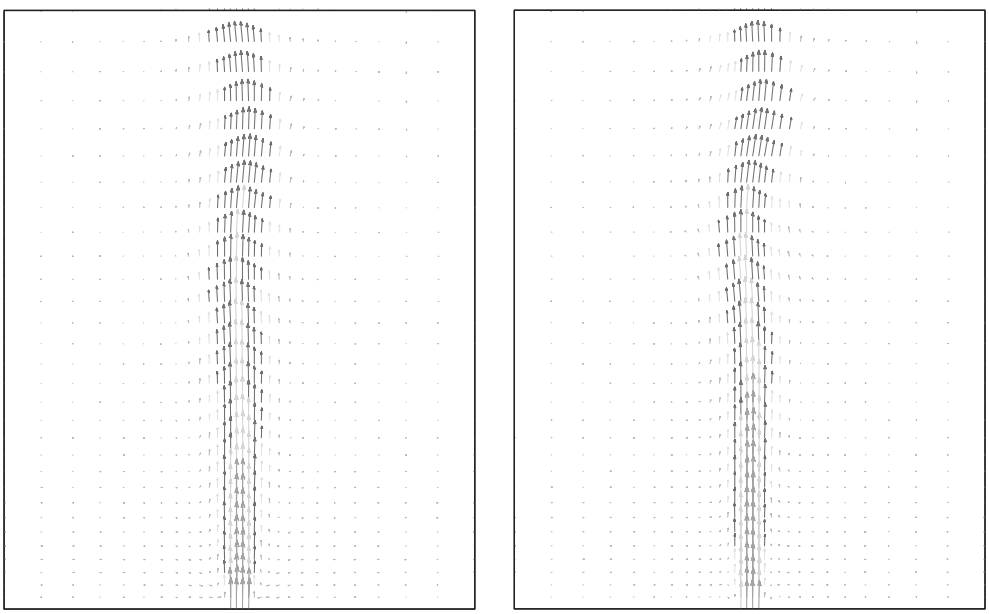


Figure 13. (a) Developed jet: a velocity vector plot in the $YZ$ plane at $X/b = 0$ and 0.041s. (b) Developed jet: a velocity vector plot in the $YZ$ plane at $X/b = 0$ and 0.042 s.

Copyright © 2002 John Wiley & Sons, Ltd. 

## 5. CONCLUSIONS

- Simple steady inlet conditions are not adequate when simulating spatially growing free shear layers. Without the use of a sophisticated turbulence inlet conditions primary results such as mean velocity decay and entrainment rates are affected. Important secondary flows may be absent from the simulation. It is readily seen and largely expected that the jet centreline mean velocity decay is strongly affected by correct turbulence conditions. The important factor for the present case is the turbulent inflow prescription which if incorrectly specified gives strongly erroneous results. The jet time mean entrainment rate is likewise affected by the specification of turbulence inlet conditions.
- A discrete method for formulating turbulence data with a known energy spectrum for an inflow boundary condition is outlined. Its implementation produces a more realistic velocity centreline decay close to the experimental results of Quinn *et al.* [9]. The division between the end of the potential core region and the start of the characteristic decay region is also clearly visible and in agreement with experiment. However, turbulent kinetic energy needs to be supplied continuously at the inlet to maintain turbulence. The use of pseudo-random noise to introduce turbulent fluctuations at the inlet is found to be insufficient.
- Off-centre mean velocity peaks are present along the major axis 10 slot widths downstream of the exit in all the simulations. The peaks are approximately 3% of the centreline velocity. The study shows that primary flow mechanisms such as the large acceleration caused by streamline curvature which are the source of the saddleback velocity profiles are not strongly affected by turbulence conditions.
- Large velocity oscillations are present in the fourth quarter of the domain (15–20 slot widths downstream) in the $y$ direction. Similar oscillations have been observed in real jets. However, these are only present for the appropriate turbulence inlet conditions. Jet flapping, which is initially caused by secondary flow phenomenon is strongly affected by turbulent inlet conditions. It is seen that the mechanism will not be excited without the presence of appropriate turbulence inlet conditions.
- To simulate three dimensional turbulent jets with a higher degree of accuracy than reported in the current study then an inflow condition which has a steady shaped mean velocity profile and a fluctuating component calculated with a known energy spectrum is desired. To observe smaller structures in the flow field the grid density needs to be increased and the time step size decreased.
- Further evidence of the effect of turbulence on secondary flow features are seen in as much as there is an imbalance between the experimentally observed Reynolds stresses and the computed Reynolds stresses downstream in the jet. Very little secondary motion is thus observed in the $xy$ plane of the numerical simulation and is attributed to the difference in the observed Reynolds stresses.

ACKNOWLEDGEMENTS

This work has been performed with the support of a grant from the Engineering and Physical Science Research Council (Marine Technology Directorate—GR/J77108/01).

Copyright © 2002 John Wiley & Sons, Ltd. 

## REFERENCES


1. Abramovich GN. *The Theory of Turbulent Jets*. MIT Press: Cambridge, MA, 1963.
2. McGuirk JJ, Rodi W. The calculation of three-dimensional turbulent free jets. In *Proceedings of the 1st Symposium on Turbulent Shear Flows*, Durst, Launder, Schmidt, Whitelaw (eds). ISBN 0-387-09041-X, 1977; 121–129.
3. Trentacoste N, Sforza P. Further experimental results for three dimensional jets. *AIAA* 1967; **5**(5):112–122.
4. Simpson BAF, Holdø AE, Byrne CEI. Large eddy simulations of high aspect ratio jets. In *Turbulence*, *Heat and Mass Transfer 2*: *Proceedings of the 2nd international symposium on Turbulence*, *Heat and Mass Transfer*, *Delft*, *Holland*, Hanjalic, Peters (eds). ISBN 90-407-1465-7, 1997; 451–460.
5. Byrne CEI, Holdø AE. Effects of increased geometric complexity on the comparison between computational and experimental simulations. *Journal of Wind Engineering and Industrial Aerodynamics* 1998; **73**(2):159–179.
6. Meares AJ, Holdø AE, Wakes SJ. A novel seeding technique for the flow visualisation of pressurized air flows. *Measurement Science and Technology* 1997; **8**(10):1183–1186.
7. Meares AJ, Holdø AE, Wakes SJ. Experimental investigation of gas leak jets relevant to offshore platforms: preliminary results. *International Maritime Technology* 1997; **109**(2):30–46.
8. (1993) FIDAP users manual version 7.6—Fluent Inc., Hampshire, USA.
9. Quinn WR, Pollard A, Marsters GF. On 'Saddle-backed' velocity distributions in three-dimensional turbulent free jets. *AIAA 16th Fluid and Plasma Dynamics Conference*, 1983.
10. Holdø AE, Weibust E. Effects due to the initial perturbations on the modelling of vortex shedding from a bluff body in a laminar flow. *Computational Fluid Dynamics* 1996; **6**:337–344.
11. Lee S, Lele SK, Moin P. Simulation of spatially evolving turbulence and the applicability of Taylors hypothesis in compressible flow. *Physics of Fluids* 1992; **A4**(7):305–321.
12. Chung YM, Sung HJ. Comparative study of inflow conditions for spatially evolving simulation. *AIAA Journal* 1997; **35**(2):161–172.
13. Pollard, Schwab RR. The near-field behaviour of rectangular free jets: an experimental and numerical study. *Proceedings of the First World Conference on Experimental Heat Transfer*, *Fluid Mechanics and Hydrodynamics*, 1988.
14. Sfeir AA. Investigation of three dimensional turbulent rectangular jets. *AIAA Journal* 1979; **4**(5):800–806.
15. Sand IØ, Sjøen K, Bakke JR. Modelling of release of gas from high pressure pipelines. *International Journal of Numerical Methods in Fluids* 1996; **23**:953–983.
16. Simpson BAF. A computational study of gas leak jets relevant to offshore installations. Ph.D. Thesis, University of Hertfordshire, England, 1998.
17. Meares AJ. An experimental study of gas leak jets relevant to offshore structures. Ph.D. Thesis, University of Hertfordshire, England, 1998.


Copyright © 2002 John Wiley & Sons, Ltd. 